

# Magnetic properties of clean surfaces of transition metals

A. V. Anisimov, V. D. Borman, L. A. Maksimov, and A. P. Popov

*Moscow Engineering-Physics Institute*

(Submitted 15 July 1991)

Zh. Eksp. Teor. Fiz. **100**, 1662–1680 (November 1991)

The magnetic structure near a surface is analyzed in the Hubbard model, which is solved in the approximation of a self-consistent field for a semi-infinite metal. A new method is proposed. It is based on a calculation of the magnetic response of a semi-infinite metal to uniform and nonuniform magnetic perturbations. It becomes possible to study the effect of a magnetic field on a semi-infinite metal and to describe the magnetic structure of the surface layers of a Cr (001) surface. At certain values of the parameters of the model, the surface magnetic moment is antiparallel to the bulk magnetic moment. The calculated results agree qualitatively with experimental results on FeNi<sub>3</sub> (111) and Gd (0001) surfaces, on which this effect was recently observed.

## 1. INTRODUCTION

In this paper we examine the magnetic structure which forms near the surface of a metal, and which is nonuniform along the normal to this surface, on the basis of the Hubbard model. We solve the problem in the self-consistent-field approximation for a semi-infinite crystal. This study was stimulated by some recent experiments on surfaces of a Permalloy-like alloy FeNi<sub>3</sub> (111) (Ref. 1) and Gd (0001) (Ref. 2), which were carried out with the help of spin-polarized electrons and the Kerr magneto-optic effect.

According to the results of those experiments, the surface magnetization of these metals is antiparallel to the magnetization of the inner regions of the sample at  $T \lesssim T_{cv}$ , where  $T_{cv}$  is the bulk value of the Curie temperature, 860 K for FeNi<sub>3</sub> and 293 K for Gd. When the temperature is lowered, the moment of the FeNi<sub>3</sub> (111) surface rotates to an orientation parallel to the moment of the interior at a certain temperature  $T_0 = 730$  K. For Gd (0001), according to the data of Ref. 3, an antiparallel orientation of the moments of the surface and inner atomic layers persists down to 200 K (the lowest temperature reached in those experiments). At  $T > T_{cv}$ , these metals retain a long-range ferromagnetic order at these faces down to the "surface Curie temperature"  $T_{cs}$ , which is  $1050 \pm 20$  K for FeNi<sub>3</sub> (111) and 315 K for Gd (0001). A long-range ferromagnetic order at the surface of a nonmagnetic metal is fairly common and is termed "surface ferromagnetism."<sup>4-8</sup> It occurs for the Tb (Ref. 9), Cr (Refs. 10 and 11), and V (Refs. 12 and 13) surfaces. The presence of at least a short-range ferromagnetic order in a surface layer has been established<sup>14</sup> for certain Ni faces.

Experiments<sup>2</sup> on Gd (0001), which were also carried out with adsorbed gases (hydrogen and oxygen) present, in amounts less than 1 L (langmuir), indicate that the surface magnetic effects outlined above disappear completely at the same temperatures. This result led Weller *et al.*<sup>2</sup> to conclude that magnetic effects at a surface involve primarily a single surface atomic layer. A factor complicating efforts to study the magnetic properties of the FeNi<sub>3</sub> (111) surface is segregation, which has been shown<sup>15</sup> to lead to a 60% enrichment of the surface atomic layer with iron. In the second atomic layer, the iron concentration is already essentially back at the stoichiometric level ( $\approx 30\%$ ). The surface ferromagne-

tism of FeNi<sub>3</sub> (111) is probably due to an enrichment of a surface atomic layer with iron, as is indicated in particular by the agreement between the surface Curie temperature of a Permalloy-like alloy,  $T_{cs} = 1050 \pm 20$  K, and the Curie temperature of bulk iron,  $T_c = 1043$  K.

If we wish to solve the problem of the magnetic structure near a surface while maintaining complete consistency from layer to layer, we must solve a system of an infinite number of equations for the electron occupation numbers  $n_{z\sigma}$  of a site in layer  $z$  ( $z = 1, 2, \dots$ ) with spins  $\sigma = \pm$ . It is rather difficult to predict at the outset just how many layers need to be taken into consideration; even if the number has been provided by experiments [as it has in the case of, e.g., Cr (100), in which this number is  $N \approx 10$  (Ref. 16)], the problem is still extremely difficult. The length scale over which a significant change in the magnetization occurs is one atomic layer, so it is not totally legitimate to switch from the discrete variable  $z$  to a continuous variable and then minimize an energy functional, as is done in the density-functional method or in the method based on the use of a Ginzburg-Landau functional with  $z$ -gradient terms. In cases in which self-consistency is imposed by means of a computer with discrete  $z$ , it is difficult to interpret the results. Furthermore, there would be strong suspicion that an inhomogeneous solution found in this manner would not be unique (Ref. 17, for example).

It thus looks worthwhile to take a slightly simplified approach. Specifically, we will determine how a semi-infinite crystal in the simple strong-coupling model responds in the linear approximation to uniform and nonuniform magnetic perturbations. These perturbations would be, for example, an external magnetic field (Sec. 2) or the magnetism of a surface atomic layer (Sec. 3). This method leans on the "approximation of one atomic layer," which itself has a somewhat shaky foundation for metals in the middle of the  $d$  series,<sup>6</sup> if the discussion is limited to them alone. However, a calculation of the magnetic response in the surface layers to a surface magnetism also yields results for Cr (which lies in the middle of the  $3d$  series) which agree qualitatively with experiments and also with other, more accurate calculations, e.g., calculations carried out by the spin-fluctuation method.<sup>16</sup> A study of the surface magnetism of Cr (100) by angle-resolved photoelectron spectroscopy with the help of synchrotron radiation has revealed that the magnetization

profile in the surface region has oscillations. These oscillations decay with distance into the crystal. Their period is the same as the lattice constant, at least near the surface; i.e., it reverses its orientation in the transition from one atomic layer to the neighboring layer.<sup>18,19</sup> As was pointed out in Ref. 19, it is the surface atomic layer of chromium which, having the maximum magnetization at  $T_N < T < T_{cs}$ , "stabilizes" the magnetic structure in the atomic layers near the surface.

The possibility of an antiparallel orientation of the surface and bulk magnetic moments of a metal along this approach is suggested by results of research on the magnetic response of surface layers to a magnetism of a surface atomic layer: It turns out that the resultant (over the layers) moment induced by the surface moment is antiparallel to this surface moment (Sec. 3) for certain positions of the Fermi level. If the temperature is lowered below the bulk Curie point, or if there is a formal increase in the Coulomb interaction in the system, the result is the appearance of a spontaneous magnetization over the entire crystal. A further result is that this effect propagates over the entire crystal; i.e., the surface moment turns out to be antiparallel not only to the resultant moment of the surface layers but also to the moments of all the inner layers (Sec. 4) which arise at  $T < T_{cv}$ .

With a further strengthening of the interaction [or with a further lowering of the temperature, as in some experiments<sup>1</sup> on FeNi<sub>3</sub> (111)], a solution corresponding to an antiparallel orientation, which exists along with the solution corresponding to a parallel orientation, disappears: The strengthened Coulomb interaction in this system and the increased bulk moment become factors which unambiguously put the surface moment in an orientation parallel to the bulk moment of the metal.

Calculations carried out below for the (100) face of a simple cube show that the change in the orientation of the surface moment occurs abruptly. The reason lies in a change in the band structure near the surface: Tamm surface states abruptly disappear. Unfortunately, the errors of the measurements<sup>1</sup> of the temperature dependence of the surface moment for FeNi<sub>3</sub> rule out a determination of whether the orientation of the surface moment changes abruptly. Answering this question will require more-careful measurements of the temperature dependence of the surface moment near  $T_0 = 730$  K and also theoretical work with a more appropriate consideration of the crystal structure of the alloy and of the indices of the face. These factors largely determine the conditions for the appearance of, and also the nature of, surface bands.<sup>20</sup>

In Sec. 2 we examine the effect of a magnetic field on a semi-infinite nonmagnetic metal. In Sec. 3 we calculate, for the surface region, the magnetic response of a metal which is nonmagnetic in its interior to a magnetism of a surface atomic layer. In Sec. 4 we examine the effect of an antiparallel orientation of the surface and bulk moments.

## 2. EFFECT OF A MAGNETIC FIELD ON A SEMI-INFINITE CRYSTAL

To describe the effects outlined above on the basis of the strong-coupling model we consider a crystal with a simple cubic lattice, consisting of  $N_1$  atomic layers  $z = 1, 2, \dots, N_1$  and a surface corresponding to the (100) face. We write the Hubbard Hamiltonian in the form

$$H = \sum_{f\sigma} \varepsilon_1 n_{f\sigma} + \sum_{f' \neq f} B_{ff'} c_{f\sigma}^\dagger c_{f'\sigma} + \frac{U}{2} \sum_{f\sigma} n_{f\uparrow} n_{f,-\sigma} - \sum_{f\sigma} \mu_z n_{f\sigma} - \sum_{f\sigma} \sigma h_z n_{f\sigma}. \quad (1)$$

Here  $\varepsilon_1$  is the energy of a one-electron atomic state,  $n_{f\sigma} = c_{f\sigma}^\dagger c_{f\sigma}$ ;  $c_{f\sigma}^\dagger$  ( $c_{f\sigma}$ ) is the operator which creates (annihilates) an electron with a spin  $\sigma = \pm$  at the site  $\mathbf{f} = (\mathbf{p}, \Delta z)$ ,  $\mathbf{p}$  is a two-dimensional vector in a layer parallel to the surface,  $B_{ff'}$  is the amplitude for the hop of an electron from site  $\mathbf{f}$  to site  $\mathbf{f}'$  (we assume that this amplitude is equal to  $B$  for sites which are nearest neighbors and zero otherwise),  $U$  is the energy of the intraatomic Coulomb repulsion of electrons with different spins, and  $\Delta$  is the interatomic distance.

For simplicity we are ignoring the dependence of the parameters  $\varepsilon_1$ ,  $B$ , and  $U$  on the distance to the surface,  $z$ . We are putting a subscript  $z$  on the chemical potential  $\mu$  and the magnetic field  $h$  to reflect the fact that these properties depend on the index of the atomic layer. We do this because we will be deriving equations for the electron occupation numbers in an atomic layer with an arbitrary  $z$  through a corresponding differentiation of the thermodynamic potential with respect to  $\mu_z$  and  $h_z$  (Sec. 4). We will then set all the  $\mu_z$  and  $h_z$  equal to each other, i.e., independent of  $z$ . In this sense the parameters of the Hamiltonian do not depend on the distance to the surface, and the variation of the resulting solutions along  $z$  stems exclusively from the fact that the crystal has a surface.

For electrons without an interaction ( $U = 0$ ) it is a simple matter to derive exact expressions for the one-particle Green's functions of layer  $z$ :

$$G_{zz}^\sigma(\varepsilon \pm i0, \mathbf{k}) = \frac{i}{2\pi N_\perp B} \frac{\sin \varphi_\sigma z}{\sin \varphi_\sigma} \exp(\mp i\varphi_\sigma z). \quad (2)$$

Here  $\mathbf{k}$  is a two-dimensional wave vector,  $\varepsilon$  is the energy, and the quantity  $\varphi_\sigma$  is determined by the relations  $\cos \varphi_\sigma = \omega_{\mathbf{k}\sigma}$ ,  $\sin \varphi_\sigma > 0$ ,  $\omega_{\mathbf{k}\sigma} = (\varepsilon - \varepsilon_\sigma)/2B - S_{\mathbf{k}}$ ,  $\varepsilon_\sigma = \varepsilon_1 - \sigma h$ , and  $S_{\mathbf{k}} = \cos k_x \Delta + \cos k_y \Delta$ . Hence we can derive expressions for the moment induced at an atom in layer  $z$ :

$$m_z = \frac{1}{\pi N_\perp B} \sum_{\mathbf{k}} \int_{-\infty}^{\varepsilon_F} d\varepsilon \left( \frac{\sin^2 \varphi_+ z}{\sin \varphi_+} - \frac{\sin^2 \varphi_- z}{\sin \varphi_-} \right). \quad (3)$$

We can also derive corresponding expressions for the susceptibilities:

$$\chi_z = \frac{2\mu_B}{\pi N_\perp B} \sum_{\mathbf{k}} \frac{\sin^2 \varphi_F z}{\sin \varphi_F}. \quad (4)$$

These susceptibilities differ only by a dimensional factor from the local density of states. The summation over  $\mathbf{k}$  in (3) and (4) is over the first Brillouin zone of the square lattice. The quantity  $\varphi_F$  is given by  $\cos \varphi_F = \omega_F - S_{\mathbf{k}}$ , where  $\omega_F = (\varepsilon_F - \varepsilon_1)/2B$ .

One can verify that in the limit  $z \rightarrow \infty$  the expression for  $\chi$  is the same as the corresponding expression which has been derived for an infinite (not semi-infinite) crystal,  $\chi_\infty$  ( $\sin^2 \varphi_F z \rightarrow 1/2$  as  $z \rightarrow \infty$ . For  $\Delta \chi_z = \chi_z - \chi_\infty$  we then have

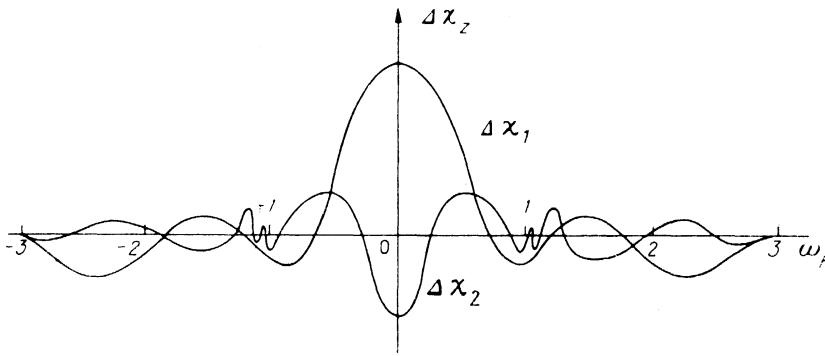


FIG. 1. Deviation of the magnetic susceptibility in the  $z$ th atomic layer from the bulk value versus the position of the Fermi level in the band of the metal.

$$\Delta\chi_z = -\frac{\mu_B}{\pi N_{\perp} B} \sum_{\mathbf{k}} \frac{\cos 2\varphi_F z}{\sin \varphi_F},$$

$$\sum_{z=1}^{\infty} \Delta\chi_z = \frac{\mu_B}{2\pi N_{\perp} B} \sum_{\mathbf{k}} \frac{1}{\sin \varphi_F} > 0. \quad (5)$$

It can be seen from (5) that the susceptibility of a semi-infinite crystal is higher than that of a bulk crystal; the effect is on the order of  $1/N_{\perp}$ . Figure 1 shows  $\Delta\chi_1$  and  $\Delta\chi_2$  versus the position of the Fermi level in the band,  $\omega_F$ . We see that under the condition  $1 < \omega_F < 2$  we have  $\Delta\chi_1 > 0$ ; i.e., for this position of the Fermi level, the surface atomic layer has a greater tendency to be in a magnetic state than the inner atomic layers do. For the same values of  $\omega_F$ , we showed in Ref. 6 that a surface ferromagnetism exists at corresponding values of the Coulomb-interaction energy  $U$ . The difference  $\Delta\chi_2$  turns out to be smaller than  $\Delta\chi_1$ , and it has the other sign at  $1 \lesssim \omega_F \lesssim 2$ . In the case  $\omega_F \approx 1$ , there are van Hove singularities, which are more prominent for  $\Delta\chi_2$  than for  $\Delta\chi_1$ . We might add that these results were derived under the assumption that there are no surface bands, in accordance with the results of Refs. 6 and 7. It was shown in those studies that surface ferromagnetism occurs in this model when surface bands are ignored. It stems from a distortion of the surface density of states in comparison with the bulk density of states.

### 3. MAGNETIZATION OF THE SURFACE LAYERS OF A METAL WITH A FERROMAGNETIC SURFACE

We now examine how a semi-infinite crystal is affected by a nonuniform perturbation consisting of a ferromagnetic state of a surface atomic layer. Our goal here is to calculate the magnetic moments at the atomic layers which lie below the surface layer and which are magnetized by this surface layer. The problem of the conditions for the appearance of a ferromagnetic state of a surface atomic layer in a metal which is nonmagnetic in its interior was solved in Ref. 6 by means of the same model which we are using here, in the approximation of a single atomic layer. We assume here that the condition that the surface is in a magnetic state, which is reached when the Coulomb interaction  $U$  exceeds a certain critical level  $U_s$  (which depends on the position of the Fermi level in the band), is satisfied. On the other hand, we assume that the extent by which  $U$  exceeds  $U_s$  is not too great. The latter assumption allows us to assume that the electron occupation numbers for the surface atoms differ only slightly from the bulk values, so we can ignore the surface bands in

the calculations and thereby simplify the problem.

The equation for the Green's function  $G_{zz}^{\sigma}(\varepsilon, \mathbf{k})$  is

$$\gamma G = \frac{i}{\pi N_{\perp} B} I, \quad \gamma_{zz} = \begin{cases} \omega - S_{\mathbf{k}} - g\delta n_{-\sigma}, & z=1, \\ \omega - S_{\mathbf{k}}, & z=2, 3, \dots, \end{cases} \quad (6)$$

$$\gamma_{zz'} = -\frac{1}{2}\delta_{z', z-1} + \gamma_{zz}\delta_{z', z} - \frac{1}{2}\delta_{z', z+1}, \quad I_{zz'} = \delta_{z, z'},$$

where  $\gamma$  and  $I$  are  $N_{\perp} \times N_{\perp}$  matrices,

$$g = U/2B, \quad \omega = (\varepsilon - \varepsilon_1)/2B - gn_0/2,$$

$$\delta n_{-\sigma} = n_{s, -\sigma} - n_0/2,$$

$n_0$  is the number of electrons per atom for an atomic layer far from the surface, and  $n_{s, -\sigma}$  is the number of electrons with a spin  $-\sigma$  for a surface atom. Using the notation  $\omega - S_{\mathbf{k}} = \cos\varphi$ , and assuming  $\sin\varphi > 0$ , we can easily derive expressions for the retarded and advanced Green's function of an arbitrary layer:

$$G_{zz}^{\sigma}(\varepsilon \pm i0, \mathbf{k}) = \frac{i}{2\pi N_{\perp} B} \frac{\sin \varphi z - \kappa_{\sigma} \sin \varphi (z-1)}{(1 - \kappa_{\sigma} e^{\mp i\varphi}) \sin \varphi} e^{\mp i\varphi z}, \quad (7)$$

$$\kappa_{\sigma} = 2g\delta n_{-\sigma},$$

We can also derive the corresponding density of states at layer  $z$ :

$$\rho_{z\sigma}(\omega) = \frac{1}{\pi N_{\perp} B} \sum_{\mathbf{k}} \frac{[\sin \varphi z - \kappa_{\sigma} \sin \varphi (z-1)]^2}{(1 - 2\kappa_{\sigma} \cos \varphi + \kappa_{\sigma}^2) \sin \varphi}. \quad (8)$$

We can thus derive expressions for the electron occupation numbers in the layer:

$$n_{z\sigma} = J_{\mathbf{k}} J_{\omega} \frac{[\sin \varphi z - \kappa_{\sigma} \sin \varphi (z-1)]^2}{(1 - 2\kappa_{\sigma} \cos \varphi + \kappa_{\sigma}^2) \sin \varphi}. \quad (9)$$

Here  $\hat{J}_{\mathbf{k}}$  and  $\hat{J}_{\omega}$  are the integral operators

$$J_{\omega}(\dots) = \int_{-\infty}^{\omega_F} d\omega(\dots), \quad J_{\mathbf{k}}(\dots) = \frac{4}{\pi^3} \int_0^{\pi} dx \int_0^{\pi} dy(\dots),$$

$$x = k_x \Delta, \quad y = k_y \Delta. \quad (10)$$

We see from (9) that if the surface is nonmagnetic, i.e., if  $n_{s+} = n_{s-}$  or  $\kappa_+ = \kappa_-$ , then we also have  $n_{z+} = n_{z-}$ , i.e.,  $m_z = 0$  for arbitrary  $z$ . If, on the other hand, the condition  $\kappa_+ \neq \kappa_-$  holds, the surface moment is  $m_s \neq 0$ , in accordance with the evolution of the band structure with distance into the crystal away from the surface. It "stabilizes" the magnetic structure near the surface, as was stated in Ref. 19. Expanding (9) in a series in the small parameter  $\kappa_{\sigma}$ , and

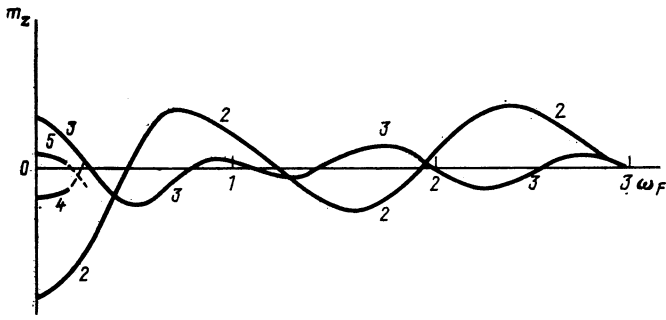


FIG. 2. Magnetic moments at the atoms of the first five atomic layers (the curve labels) induced by a magnetic surface versus the position of the Fermi level in the metal band.

using only the linear approximation, we find expressions for the moments induced by the magnetic surface at an arbitrary layer  $z$ . After an integration over the energies  $\omega$ , the expression for  $m_z = n_{z+} - n_{z-}$  becomes

$$m_z = g m_s j_k \left[ \frac{\sin \varphi_F (2z-1)}{2z-1} - \frac{\sin \varphi_F (2z+1)}{2z+1} \right], \quad (11)$$

$$\varphi_F = \arccos \left( \frac{\varepsilon_F - \varepsilon_1}{2B} - g n_0 / 2 - S_k \right).$$

It is also a simple matter to calculate the resultant moment  $m_\Sigma$  induced by the magnetic surface (the resultant over the layers):

$$m_\Sigma = \sum_{z=2}^{\infty} m_z = g m_s j_k \frac{\sin 3\varphi_F}{3}. \quad (12)$$

Figure 2 shows curves of  $m_z$  versus the position of the Fermi level in the band; here  $\omega_F$  represents the quantity

$$(\varepsilon_F - \varepsilon_1) / 2B - g n_0 / 2.$$

We see that if the Fermi level lies near the middle of the band the moments induced at the layers near the surface by a magnetic surface change sign from one atomic layer to the next. The adherence to this behavior is stricter, the closer the Fermi level to the middle of the band. As we mentioned in the Introduction, this behavior has been observed experimentally<sup>18,19</sup> at temperatures above the Néel point  $T_N$  in the surface layers of Cr, which is in the middle of the 3d series.

Figure 3 shows the behavior of the resultant (over the layers) moment induced by a magnetic surface,  $m_\Sigma$ , as a function of the Fermi energy  $\omega_F$ . We see from this figure that we have  $m_\Sigma < 0$  near the middle of the band and—the more important point—that this condition also holds at  $1 < \omega_F < 2$ , i.e., at values of  $\omega_F$  for which a surface ferromagnetism occurs. A magnetic surface thus creates a resultant moment of the opposite sign near the surface. This result suggests at the very least that an antiparallel orientation of the surface and bulk magnetic moments is possible upon the appearance of a spontaneous magnetization in the interior. This coincidence of the  $\omega_F$  intervals in which the surface ferromagnetism occurs and in which the condition  $m_\Sigma < 0$  holds also suggests that metals for which surface ferromagnetism occurs probably also have an antiparallel orientation of the bulk and surface moments. This combination has been manifested in experiments<sup>1,2</sup> on FeNi<sub>3</sub> (111) and Gd (0001).

To conclude this section we note that we have made no special assumptions regarding an antiferromagnetic struc-

ture of the surface region. In this regard our method differs from previous calculations, e.g., by the spin-fluctuation method,<sup>16</sup> which is apparently the most appropriate method for describing the magnetic properties of transition metals. The question of a ground state thus does not arise. Furthermore, we have placed no restriction on the number ( $N$ ) of layers incorporated in the self-consistent calculations, and the properties of these layers have been assumed to differ from those of the bulk layers ( $N = 10$  was assumed in Ref. 16).

#### 4. ANTIPARALLEL ORIENTATION OF THE SURFACE AND BULK MOMENTS OF A METAL

In this section of the paper we show that a state with antiparallel surface and bulk moments can arise as a solution of a system of equations for the corresponding occupation numbers. Such a state is favored from the energy standpoint for certain values of the parameters of the model—values which are characteristic of FeNi<sub>3</sub>. For simplicity we will ignore the segregation-induced differences between the parameter values of the model for the surface and the interior. This would correspond better to the experimental situation regarding FeNi<sub>3</sub> (111) in Ref. 1. We will show that an antiparallel orientation of the surface and bulk moments can also occur when the values of these parameters are the same. To reach our goal, we again use Hamiltonian (1), now assuming that the inner layers of the metal can be in a magnetic state. The difference between the surface and bulk occupation numbers can then be substantial, and there is no justification for excluding surface bands from the analysis. Since an entire set of possible magnetic surface states is realized in this section, in contrast with the preceding sections of this paper, we must compare the thermodynamic potentials corresponding to these states in order to decide which is the ground state. We will accordingly not use the Green's-function method. We will instead calculate the thermodynamic

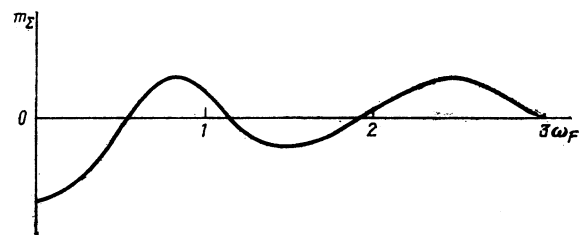


FIG. 3. Resultant value, over the layers, of the magnetic moment induced by a magnetic surface in a nonmagnetic metal ( $U = 0$ ) versus the position of the Fermi level in the metal band.

potential of the metal by solving the eigenvalue problem for Hamiltonian (1) for a semi-infinite crystal.

Considering only magnetic states which are uniform along the surface, we take two-dimensional Fourier transforms in Hamiltonian (1). In the approximation of a self-consistent field we then find

$$H = 2B \left\{ -gN_{\perp} \sum_{z=1}^{N_{\perp}} n_{z+} n_{z-} + \sum_{z,z'=1}^{N_{\perp}} \sum_{\mathbf{k}\sigma} \hat{c}_{z'\mathbf{k}\sigma}^{\dagger} \hat{\rho}_{z'\mathbf{k}\sigma}^{\sigma}(\mathbf{k}) \hat{c}_{z\mathbf{k}\sigma} \right\},$$

$$\hat{\rho}_{z'\mathbf{k}\sigma}^{\sigma}(\mathbf{k}) = \frac{1}{2} \delta_{z',z-1} + \omega_{z\mathbf{k}\sigma} \delta_{z',z} + \frac{1}{2} \delta_{z',z+1}, \quad (13)$$

$$\omega_{z\mathbf{k}\sigma} = \begin{cases} \omega_{s\mathbf{k}\sigma}, & z=1, \\ -\omega_{\mu\mathbf{k}\sigma}, & z=2, 3, \dots, \end{cases}$$

$$\omega_{s\mathbf{k}\sigma} = 2B(\epsilon_s + Un_{s,-\sigma} - \mu_s - \sigma h_s - S_{\mathbf{k}}),$$

$$-\omega_{\mu\mathbf{k}\sigma} = 2B(\epsilon_v + Un_{v,-\sigma} - \mu_v - \sigma h_v - S_{\mathbf{k}}).$$

It is convenient to break  $\omega_{s\mathbf{k}\sigma}$  up into two parts:

$$\omega_{s\mathbf{k}\sigma} = -\omega_{\mu\mathbf{k}\sigma} + \delta\omega_{\sigma},$$

$$\delta\omega_{\sigma} = \frac{1}{2B} [(\epsilon_s - \epsilon_v) + U(n_{s,-\sigma} - n_{v,-\sigma}) - (\mu_s - \mu_v) - \sigma(h_s - h_v)], \quad (14)$$

$$\omega_{\mu\mathbf{k}\sigma} = \omega_{\mu} - gn_{v,-\sigma} - S_{\mathbf{k}} - \sigma h_v, \quad \omega_{\mu} = (\mu_v - \epsilon_v)/2B.$$

In accordance with the discussion above, all the quantities in  $\delta\omega_{\sigma}$  which correspond to the interior and the surface are set equal, except for  $n_{s,-\sigma}$  and  $n_{v,-\sigma}$ , which we intend to find in a self-consistent way. We will refer to  $\omega_{\mu}$  as the "Fermi energy" or "chemical potential." The first term in (13) is simply a number, since it contains nothing but expectation values of  $n_{z\pm}$ . The equation for the eigenvalues  $\Lambda$  of Hamiltonian (13) can thus be written

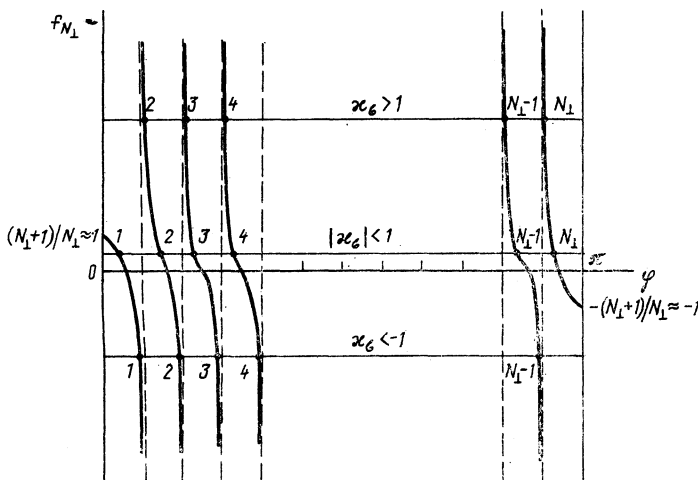
$$\det \left\| -\frac{1}{2} \delta_{z',z-1} + (\Lambda - \omega_{z\mathbf{k}\sigma}) \delta_{z',z} - \frac{1}{2} \delta_{z',z+1} \right\| = 0. \quad (15)$$

The solutions of Eq. (15) differ substantially in the three cases  $|\Lambda + \omega_{\mu\mathbf{k}\sigma}| \leq 1$ ,  $\Lambda + \omega_{\mu\mathbf{k}\sigma} > 1$  and  $\Lambda + \omega_{\mu\mathbf{k}\sigma} < -1$ .

Let us consider each case separately. If  $|\Lambda + \omega_{\mu\mathbf{k}\sigma}| < 1$ , then by introducing  $\Lambda + \omega_{\mu\mathbf{k}\sigma} = \cos\varphi$  and assuming  $\sin\varphi > 0$  we can rewrite Eq. (15) as

$$\sin\varphi(N_{\perp} + 1) - \kappa_{\sigma} \sin\varphi N_{\perp} = 0, \quad \kappa_{\sigma} = 2\delta\omega_{\sigma}, \quad (16)$$

or



$$f_{N_{\perp}}(\varphi) = \frac{\sin\varphi(N_{\perp} + 1)}{\sin\varphi N_{\perp}} = \kappa_{\sigma}.$$

Figure 4 shows a plot of the function  $f_{N_{\perp}}(\varphi)$ . We see that under the condition  $|\kappa_{\sigma}| \leq (N_{\perp} + 1)/N_{\perp} \approx 1$ , Eq. (16) has  $N_{\perp}$  roots on the interval  $[0, \pi]$ , while if the condition  $|\kappa_{\sigma}| > (N_{\perp} + 1)/N_{\perp}$  holds Eq. (16) has  $N_{\perp} - 1$  roots on this interval. In other words, if  $|\kappa_{\sigma}| > 1$ , then surface bands appear. These bands are discussed below under the assumption  $\Lambda + \omega_{\mu\mathbf{k}\sigma} > 1$  or  $\Lambda + \omega_{\mu\mathbf{k}\sigma} < -1$ . The problem of finding the eigenvalues of Eq. (16) was solved in Ref. 8 by a method of successive approximations in the small parameter  $\kappa_{\sigma}$ . In other words, the assumption  $|\kappa_{\sigma}| \ll 1$  was used. It was shown in particular that all the corrections to the Taylor series in  $\kappa_{\sigma}$  for  $\Lambda$  are small quantities on the order of  $1/(N_{\perp} + 1)$ . In the present paper we have succeeded in deriving an analytic expression for the eigenvalues  $\Lambda$  by making use of the small quantity  $1/(N_{\perp} + 1)$ , without the further assumption that the quantity  $\kappa_{\sigma}$  is small. In other words, we write

$$\Lambda \approx \Lambda_{0\mathbf{k}q\sigma} + \frac{1}{N_{\perp} + 1} \Lambda_{1\mathbf{k}q\sigma},$$

$$\Lambda_{0\mathbf{k}q\sigma} = -\omega_{\mu\mathbf{k}\sigma} + \cos\varphi_q, \quad \varphi_q = \frac{\pi q}{N_{\perp} + 1}, \quad q = 1, 2, \dots, N_{\perp}, \quad (17)$$

$$\Lambda_{1\mathbf{k}q\sigma} = \sin\varphi_q \left[ \operatorname{arctg} \frac{\kappa_{\sigma} \sin\varphi_q}{1 - \kappa_{\sigma} \cos\varphi_q} + \begin{cases} \pi\theta(\kappa_{\sigma} - 1)\theta\left(\arccos\frac{1}{\kappa_{\sigma}} - \varphi_q\right) \\ -\pi\theta(-\kappa_{\sigma} - 1)\theta\left(\varphi_q - \arccos\frac{1}{\kappa_{\sigma}}\right) \end{cases} \right],$$

where  $\theta(\kappa)$  is the unit step function.

We now assume  $\Lambda + \omega_{\mu\mathbf{k}\sigma} > 1$ . Using the notation  $\Lambda + \omega_{\mu\mathbf{k}\sigma} = \chi\varphi$ , and assuming  $\sin\varphi > 0$ , we find Eq. (15) in

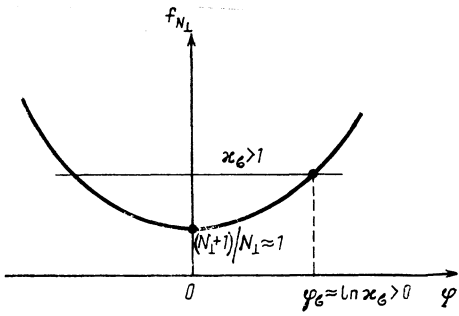


FIG. 5. Graphical solution of Eq. (18). At  $\kappa_\sigma > 1$ , there is one solution, which satisfies the condition  $\varphi_\sigma > 0$  and which corresponds to a surface band  $\rho_{s\sigma}^+(\omega)$ .

the form

$$\text{sh } \varphi(N_\perp + 1) - \kappa_\sigma \text{sh } \varphi N_\perp = 0. \quad (18)$$

For  $\varphi > 0$ , this equation has roots only under the condition  $\kappa_\sigma > +1$ . Figure 5 shows curves of  $f_{N_1}(\varphi) = \text{sh}\varphi(N_\perp + 1)/\text{sh}\varphi N_\perp$ . Taking the limit  $N_1 \rightarrow \infty$ , we find  $f_{N_1}(\varphi) \rightarrow e^\varphi$ . In other words, the eigenvalue found in this case can be written in the form

$$\Lambda_{s\mathbf{k}\sigma}^+ = -\omega_{\mu\mathbf{k}\sigma} + \frac{\kappa_\sigma^2 + 1}{2\kappa_\sigma}, \quad \kappa_\sigma > 1. \quad (19)$$

If  $\Lambda + \omega_{\mu\mathbf{k}\sigma} < -1$ , then by introducing the notation  $\Lambda + \omega_{\mu\mathbf{k}\sigma} = -\text{ch}\varphi$  and assuming  $\text{sh}\varphi > 0$ , we find the equation

$$\text{sh}\varphi(N_\perp + 1) + \kappa_\sigma \text{sh}\varphi N_\perp = 0,$$

in the corresponding way. This equation has a solution only under the condition  $\kappa_\sigma < -1$ :

$$\Lambda_{s\mathbf{k}\sigma}^- = -\omega_{\mu\mathbf{k}\sigma} + \frac{\kappa_\sigma^2 + 1}{2\kappa_\sigma}, \quad \kappa_\sigma < -1. \quad (20)$$

Hamiltonian (13) can thus be written in diagonal form, with an accuracy to  $1/(N_\perp + 1)^2$ , by going over from the  $z$  representation of (3) to the  $q$  representation:

$$H = 2B \left\{ -gN_\parallel \sum_{z=1}^{N_\perp} n_z \cdot n_z - \sum_{\mathbf{k}\sigma} \left[ \sum_{q=1}^{N_\perp} \left( \Lambda_{0\mathbf{k}q\sigma} + \frac{1}{N_\perp + 1} \Lambda_{1\mathbf{k}q\sigma} \right) \hat{n}_{\mathbf{k}q\sigma} + \Lambda_{s\mathbf{k}\sigma}^+ \hat{n}_{s\mathbf{k}1\sigma} \theta(\kappa_\sigma - 1) + \Lambda_{s\mathbf{k}\sigma}^- \hat{n}_{s\mathbf{k}N_\perp\sigma} \theta(-\kappa_\sigma - 1) \right] \right\}. \quad (21)$$

The operators  $\hat{n}_{s\mathbf{k}1\sigma}$  and  $\hat{n}_{s\mathbf{k}N_\perp\sigma}$  correspond to surface bands, i.e., to the first or  $N_\perp$ th value of  $q$ , which specifies the particular root of Eq. (15) under the condition  $\kappa_\sigma > +1$  or  $\kappa_\sigma < -1$ . The summation over  $q$  in the second term in (21) should be carried out under the condition that the total number of states is conserved. In other words, if  $\kappa_\sigma > +1$ , then  $2 \leq q \leq N_\perp$ , and if  $\kappa_\sigma < -1$  then  $1 \leq q \leq N_\perp - 1$ . This approach reflects the introduction of the primed sum over  $q$  in (21). We might add that the last two terms in (21) are not mutually exclusive, since the case with  $\kappa_+ > +1$  and  $\kappa_- < -1$  or with  $\kappa_+ < -1$  and  $\kappa_- > +1$  is possible. In other words,

there is the possibility in principle of a situation with two surface bands.

Using (17), (19), and (20), we write an expression for the thermodynamic potential  $\Omega$  at finite temperatures  $T$ :

$$\Omega = 2B \left\{ -gN_\parallel (n_s + n_{s-} - n_{v+} + n_{v-}) - gN_\parallel N_\perp n_{v+} + n_{v-} - t \sum_{\mathbf{k}\sigma} \left\{ \sum_q' \ln \left[ 1 + \exp \left( - \frac{\Lambda_{0\mathbf{k}q\sigma} + \Lambda_{1\mathbf{k}q\sigma} / (N_\perp + 1)}{t} \right) \right] + \ln \left[ 1 + \exp \left( - \frac{\Lambda_{s\mathbf{k}\sigma}^+}{t} \right) \right] \theta(\kappa_\sigma - 1) + \ln \left[ 1 + \exp \left( - \frac{\Lambda_{s\mathbf{k}\sigma}^-}{t} \right) \right] \theta(-\kappa_\sigma - 1) \right\} \right\}. \quad (22)$$

where  $t = T/2B$ . Introducing

$$\sum_{\mathbf{k}} (\dots) = N_\parallel \frac{2}{\pi^2} \int_0^\pi dx \int_0^\pi dy (\dots) = N_\parallel \hat{J}_{\mathbf{k}} (\dots),$$

$$\sum_{q=1}^{N_\perp} (\dots) \approx (N_\perp + 1) \frac{1}{\pi} \int_0^\pi d\varphi (\dots) = (N_\perp + 1) \hat{J}_\varphi (\dots)$$

and taking the limit  $t \rightarrow 0$ , we find an expression for the thermodynamic potential of a semi-infinite crystal at absolute zero. This expression is broken up into a volume part ( $\propto N_\parallel N_\perp$ ) and a surface part ( $\propto N_\parallel$ ):

$$\Omega = \Omega_v + \Omega_s,$$

$$\Omega_v = 2BN_\parallel N_\perp \left[ -gn_{v+} + n_{v-} + J_{\mathbf{k}} J_\varphi \sum_{\sigma} \Lambda_{0\mathbf{k}q\sigma} \theta(-\Lambda_{0\mathbf{k}q\sigma}) \right], \quad (23)$$

$$\Omega_s = 2BN_\parallel \left[ -g(n_s + n_{s-} - n_{v+} + n_{v-}) + J_{\mathbf{k}} J_\varphi \sum_{\sigma} \Lambda_{1\mathbf{k}q\sigma} \theta(-\Lambda_{0\mathbf{k}q\sigma}) + J_{\mathbf{k}} \sum_{\sigma} \Lambda_{s\mathbf{k}\sigma}^+ \theta(-\Lambda_{s\mathbf{k}\sigma}^+) \theta(\kappa_\sigma - 1) + J_{\mathbf{k}} \sum_{\sigma} \Lambda_{s\mathbf{k}\sigma}^- \theta(-\Lambda_{s\mathbf{k}\sigma}^-) \theta(-\kappa_\sigma - 1) - J_{\mathbf{k}} \sum_{\sigma} (\Lambda_{0\mathbf{k}1\sigma} \theta(-\Lambda_{0\mathbf{k}1\sigma}) \theta(\kappa_\sigma - 1) + \Lambda_{0\mathbf{k}N_\perp\sigma} \theta(-\Lambda_{0\mathbf{k}N_\perp\sigma}) \theta(-\kappa_\sigma - 1)) \right]$$

We introduce

$$\Omega_s^\pm = 2BN_\parallel J_{\mathbf{k}} \sum_{\sigma} \Lambda_{s\mathbf{k}\sigma}^\pm \theta(-\Lambda_{s\mathbf{k}\sigma}^\pm) \theta(|\kappa_\sigma| - 1). \quad (24)$$

We can also write an expression for the function representing the density of surface states, which we found by a Green's-function method and which consists of three contributions:

$$\rho_{s\sigma}(\omega) = \rho_{s\sigma}^{(0)} + \rho_{s\sigma}^+ + \rho_{s\sigma}^-,$$

The last two of these components exist by virtue of the existence of surface bands. Here

$$\begin{aligned} \rho_{s\sigma}^{(0)}(\omega) &= \frac{1}{\pi B} \hat{J}_k \frac{(1-\omega_{k\sigma}^2)^{1/2}}{1-2\kappa_\sigma\omega_{k\sigma}+\kappa_\sigma^2}, \quad |\omega_{k\sigma}| < 1, \\ \rho_{s\sigma^+}(\omega) &= \frac{1}{B} \hat{J}_k \frac{\kappa_\sigma^2-1}{2\kappa_\sigma^2} \delta(\omega_{k\sigma}-\omega_\sigma^{(0)}), \quad \omega_{k\sigma} > 1, \\ \rho_{s\sigma^-}(\omega) &= \frac{1}{B} \hat{J}_k \frac{\kappa_\sigma^2-1}{2\kappa_\sigma^2} \delta(\omega_{k\sigma}-\omega_\sigma^{(0)}), \quad \omega_{k\sigma} < -1, \\ \omega_\sigma^{(0)} &= \frac{\kappa_\sigma^2+1}{2\kappa_\sigma}, \quad \omega_{k\sigma} = \omega - gn_{v,-\sigma} - S_k. \end{aligned} \quad (25)$$

We will need these expressions in order to determine the spectrum of the surface band structure. Equations for the occupation numbers of the surface,  $n_{s\sigma} = n_{s\sigma}^{(0)} + n_{s\sigma}^+ + n_{s\sigma}^-$ , are found through an appropriate differentiation of the thermodynamic potential  $\Omega_s$  or through an integration of (25). We write the contributions  $n_{s\sigma}$  from the surface bands separately:

$$\begin{aligned} n_s^+ &= n_{s^+}^+ + n_{s^+}^- = -\frac{1}{N_{\parallel}} \left. \frac{\partial \Omega_s^+}{\partial \mu_s} \right|_{\mu_s = \mu_v} \\ &= 2\hat{J}_k \sum_{\sigma} \frac{\kappa_\sigma^2-1}{2\kappa_\sigma^2} \frac{\theta(\kappa_\sigma-1)}{\exp(\Lambda_{sk\sigma}^+/t) + 1}, \\ n_s^- &= n_{s^-}^+ + n_{s^-}^- = -\frac{1}{N_{\parallel}} \left. \frac{\partial \Omega_s^-}{\partial \mu_s} \right|_{\mu_s = \mu_v} \\ &= 2\hat{J}_k \sum_{\sigma} \frac{\kappa_\sigma^2-1}{2\kappa_\sigma^2} \frac{\theta(-\kappa_\sigma-1)}{\exp(\Lambda_{sk\sigma}^-/t) + 1}. \end{aligned} \quad (26)$$

Correspondingly, for the part of the surface moment associated with the surface bands we find

$$\begin{aligned} m_s^+ &= n_{s^+}^+ - n_{s^+}^- = -\frac{1}{N_{\parallel}} \left. \frac{\partial \Omega_s^+}{\partial h_s} \right|_{h_s=0} \\ &= 2\hat{J}_k \sum_{\sigma} \frac{\kappa_\sigma^2-1}{2\kappa_\sigma^2} \frac{\sigma\theta(\kappa_\sigma-1)}{\exp(\Lambda_{sk\sigma}^+/t) + 1}, \\ m_s^- &= n_{s^-}^+ - n_{s^-}^- = -\frac{1}{N_{\parallel}} \left. \frac{\partial \Omega_s^-}{\partial h_s} \right|_{h_s=0} \\ &= 2\hat{J}_k \sum_{\sigma} \frac{\kappa_\sigma^2-1}{2\kappa_\sigma^2} \frac{\sigma\theta(-\kappa_\sigma-1)}{\exp(\Lambda_{sk\sigma}^-/t) + 1}. \end{aligned} \quad (27)$$

In the limit  $t \rightarrow 0$  we then find

$$\begin{aligned} n_{s\sigma^+} &= 2 \frac{\kappa_\sigma^2-1}{2\kappa_\sigma^2} \hat{J}_k \theta(-\Lambda_{sk\sigma}^+) \theta(\kappa_\sigma-1), \\ n_{s\sigma^-} &= 2 \frac{\kappa_\sigma^2-1}{2\kappa_\sigma^2} \hat{J}_k \theta(-\Lambda_{sk\sigma}^-) \theta(-\kappa_\sigma-1). \end{aligned} \quad (28)$$

It can be seen from these expressions that a surface-band contribution to the occupation numbers exists only for  $\kappa_\sigma > +1$  in the case of  $n_{s\sigma}^+$  or for  $\kappa_\sigma < -1$  in the case of  $n_{s\sigma}^-$ . The expressions found for  $n_{s\sigma}^\pm$  through the integration of the density of states in (25) are the same as those given in (28), as they should be. The expression for  $n_{s\sigma}^{(0)}$  is

$$n_{s\sigma}^{(0)} = \frac{2}{\pi} \hat{J}_k \hat{J}_\omega \frac{(1-\omega_{k\sigma}^2)^{1/2}}{1-2\kappa_\sigma\omega_{k\sigma}+\kappa_\sigma^2}. \quad (29)$$

Adding (28) and (29), we find a system of equations for the electron occupation numbers of a surface atom,  $n_{s^+}$  and  $n_{s^-}$ . This system of equations must be solved jointly with the system of equations for the electron occupation

numbers for an atom from an interior layer of the metal,  $n_{v\sigma}$ :

$$n_{v\sigma} = \frac{1}{2} \hat{J}_k (\pi - \arccos \omega_{\mu k \sigma}), \quad (30)$$

The reason is that the quantity  $\kappa_\sigma = 2g(n_{s,-\sigma} - n_{v,-\sigma})$  appears in (28) and (29).

Unfortunately, in solving Eqs. (28)–(30) for the electron occupation numbers of a surface atom,  $n_{s^+}$  and  $n_{s^-}$ , we cannot use an expansion in  $\kappa_\sigma$ , since to do so would immediately cause the formal disappearance of the surface bands. In addition, a joint numerical solution of Eqs. (28)–(30) leads, for certain values of the interaction  $j = U/W$  ( $W = 12B$  is the width of the band of the metal), to magnetic solutions which correspond to  $|\kappa_\sigma| > +1$ . In other words, surface bands would in fact exist. Figure 6a shows curves of the magnetic moments of surface atoms,  $m_s$ , and of bulk atoms,  $m_v$ , versus  $j$  for various solutions; the corresponding thermodynamic potentials  $\Omega_s$  for absolute zero are shown in Fig. 6b.

Figure 7 illustrates the graphical method used to solve the system of equations for  $n_{s^+}$  and  $n_{s^-}$ . In other words, this figure shows  $n_{s^+}$  versus  $n_{s^-}$  and also  $n_{s^-}$  versus  $n_{s^+}$  for various values of the interaction  $j$ . At sufficiently small values  $j < j_s$ , the surface and the interior are nonmagnetic: The  $n_{s^+}$  ( $n_{s^-}$ ) and  $n_{s^-}$  ( $n_{s^+}$ ) curves have only one intersection point, on the diagonal ( $n_{s^+} = n_{s^-}$ ) of the unit square  $0 \leq n_{s^\pm} \leq 1$ . This case is trivial and is therefore omit-

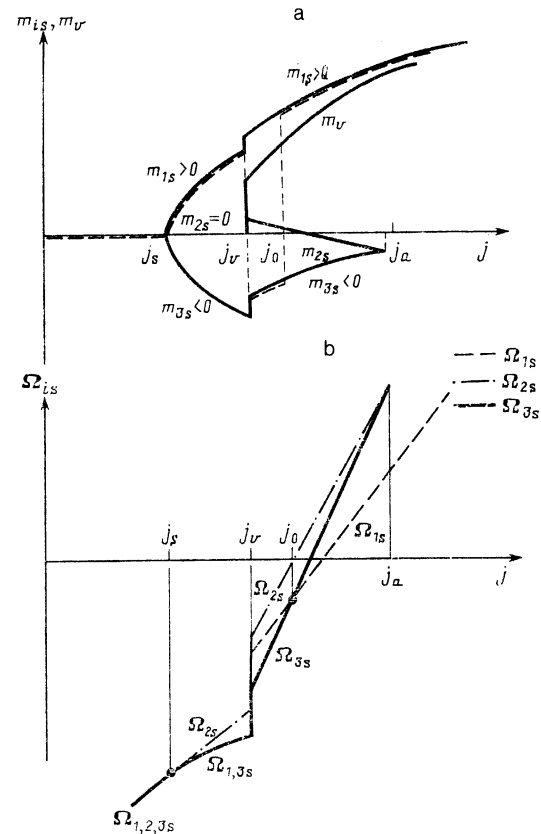


FIG. 6. a: Magnetic moments corresponding to the first, second, and third solution for the surface versus the interaction  $j$ . The dashed line shows the surface moment realized in a weak magnetic field  $h > 0$ . b: Thermodynamic potentials corresponding to the first, second, and third solutions at  $T = 0$  for the surface versus the interaction  $j$ . Under the conditions  $j_0 < j < j_a$ , the preferred solution has an antiparallel orientation of the surface and bulk moments, because of the relations  $\Omega_{3s} < \Omega_{2s}, \Omega_{1s}$ .

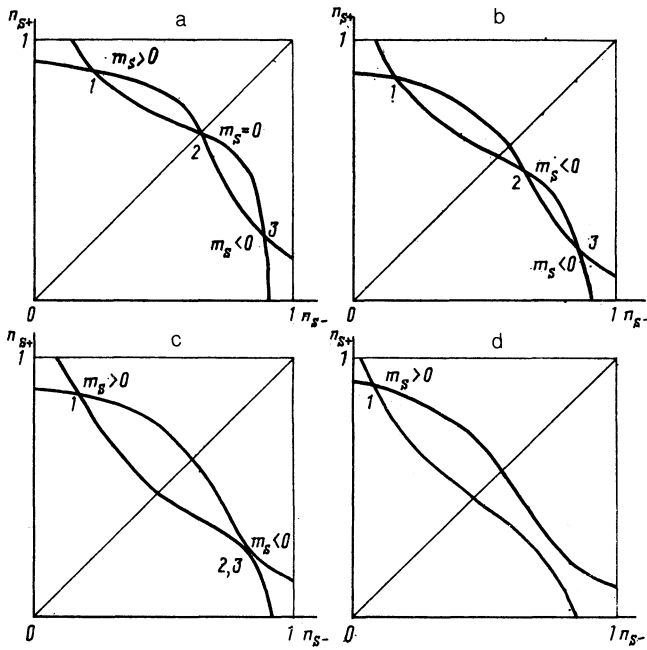


FIG. 7. Graphical solution of the equations for the electron occupation numbers  $n_{s+}$  and  $n_{s-}$  of a surface atom. a:  $j_s < j < j_v$ . There are two magnetic solutions (1 and 3) and one nonmagnetic solution (2),  $m_{3s} = -m_{1s}$ . b:  $j_v < j < j_a$ . Solution 2 has become magnetic. The points corresponding to solutions 2 and 3 approach each other with increasing  $j$ . c:  $j = j_a$ . Solutions 2 and 3 have become coincident.  $m_{2,3s} < 0$ . d:  $j > j_a$ . Solutions 2 and 3 with  $m_s < 0$  have disappeared. Only solution 1, with  $m_s > 0$ , remains.

ted from Fig. 7. When the strength of the interaction reaches  $j = j_s + 0$ , the surface can be in either of two states, which are designated 1 and 3 in Fig. 7. Corresponding to state 1 is a moment  $m_{1s} > 0$ , and corresponding to state 3 is  $m_{3s} < 0$ . State 2 is nonmagnetic under the conditions  $j_s < j < j_v$  ( $m_{2s} = 0$ ). With increasing  $j$ , the magnetic states appear smoothly, without discontinuities; i.e., a second-order phase transition occurs at the surface. In the interior, we have  $m_v = 0$ , as before; i.e., we find a surface ferromagnetism. This effect cannot occur at arbitrary values of the Fermi energy.<sup>6</sup> The curves in Figs. 6 and 7 were constructed for  $\omega_\mu = 6$ .

By virtue of the symmetry under time reversal, the state with a magnetic surface is degenerate with respect to the orientation of the moment  $m_{3s} = -m_{1s} < 0$  and also  $\Omega_{1s} = \Omega_{3s}$  under the conditions  $j_s < j < j_v$  (Fig. 6b). Here we have  $\Omega_{2s} > \Omega_{1,3s}$ . At  $j > j_v$ , a moment  $m_v \neq 0$  appears in the interior. As can be seen from Fig. 6a, this event occurs through a first-order phase transition. This conclusion does not agree with the experimental situation, since the bulk magnetism appears in FeNi<sub>3</sub> through a second-order phase transition.

In principle, the Hubbard model also allows the appearance of a bulk moment through a second-order phase transition, at, for example,  $\omega_\mu = 9$ . This point is not of really fundamental importance, however, since a search for solutions which are magnetic for the interior in the Hubbard model in the mean-field approximation should be regarded as basically a modeling of bulk magnetism followed by a resolution of the question of the state of the surface. The more favorable magnetic solution for the interior is also degenerate with

respect to the orientation of the moment. Let us assume that we have turned on an infinitely weak field  $h > 0$ . Under the conditions  $j_s < j < j_v$ , there will then be a magnetic state at the surface with  $m_{1s} > 0$ . At  $j > j_v$ , of the two magnetic solutions for the interior,  $m_v \geq 0$ , the state with  $m_v > 0$  will be realized. The latter conclusion is correct because the correction to the bulk solutions for the presence of a surface, which we are ignoring, is on the order of  $1/N_1$ . The question of the surface state is thus solved for an unambiguously given bulk state ( $m_v > 0$ ).

When a bulk magnetism ( $j > j_v$ ) arises, the symmetry (with respect to the diagonal  $n_{s+} = n_{s-}$ ) in the positions of the magnetic solutions for the surface is disrupted, as can be seen from Figs. 7a and 7b. Points 1 and 3, which correspond to a magnetic solution for the surface with  $m_{1s} > 0$  and  $m_{3s} < 0$ , begin to move toward the upper left corner in Fig. 7b with an increase in  $j$  and with a consequent increase in the bulk moment,  $m_v(j) > 0$ . In other words, the moment  $m_{1s} > 0$  increases, while the moment  $m_{3s} < 0$  decreases in magnitude, while remaining negative; i.e., the increasing bulk moment  $m_v > 0$  magnetizes the surface in its own direction. Solution 2, which was nonmagnetic in the case  $j < j_v$ , initially moves away from the diagonal  $n_{s+} = n_{s-}$  upward, in an abrupt jump. It then descends smoothly, intersects the diagonal, and takes a position below the diagonal at sufficiently large values of  $j$  (Fig. 6a). Points 2 and 3 in Fig. 7b thus move toward each other with increasing  $j > j_v$ .

When the interaction  $j$  reaches a certain critical value  $j_a$ , the points corresponding to solutions 2 and 3 coincide. This coincidence corresponds to a tangency of the curves in Fig. 7c. The moment corresponding to them remains negative (Fig. 6a). Finally, at  $j > j_a$  the curves intersect just once: Solutions 2 and 3 disappear, and we are left with only solution 1, with  $m_{1s} > 0$  (Fig. 7d). It can be seen from Fig. 6b that the magnetic solution with a negative moment for the surface corresponds to a lower thermodynamic potential for the magnetic interior,  $\Omega_{3s} < \Omega_{1s}$ ,  $\Omega_{2s}$ , under the conditions  $j_v < j < j_0$ . The switch from solution 3 with  $m_s < 0$  to solution 1 with  $m_s > 0$  at the point  $j = j_0$  is accompanied (Fig. 6a) by an abrupt change in the magnitude and sign of the surface moment. The dashed line in Fig. 6a shows the behavior of the surface moment which is realized in a weak magnetic field as the interaction  $j$  increases.

Figure 8 shows curves of the "phase boundaries"  $j_s, j_v$ , and  $j_0$  versus the temperature. The critical value increases with increasing temperature.<sup>6</sup> The quantity  $j_v$  also increases with the temperature. In this case  $j_s(T)$  does not intersect  $j_v(T)$ , although for certain positions of  $\omega_\mu$  the  $j_v(T)$  curves can have a shallow minimum.<sup>21</sup> The quantity  $j_0$  apparently also increases with the temperature. We now consider a semi-infinite crystal with  $j > j_0$  at  $T \neq 0$ . At low temperatures  $T < T_0$ , the surface and the interior are magnetized in parallel; i.e., we have  $m_s > 0$ . When the temperature reaches the value  $T_0$ , which is the root of the equation  $j = j_0(T)$ , the interaction  $j$  becomes smaller than  $j_0(T)$  at  $T > T_0$ . In this case (Fig. 6a), the surface moment changes abruptly in value, going negative at  $T_0 < T < T_{cv}$  (Fig. 8b). With a further increase in the temperature, the magnetic moment decreases at the Curie point  $T_{cv}$ , and the surface moment becomes positive again, since the interaction  $j$  becomes weaker than

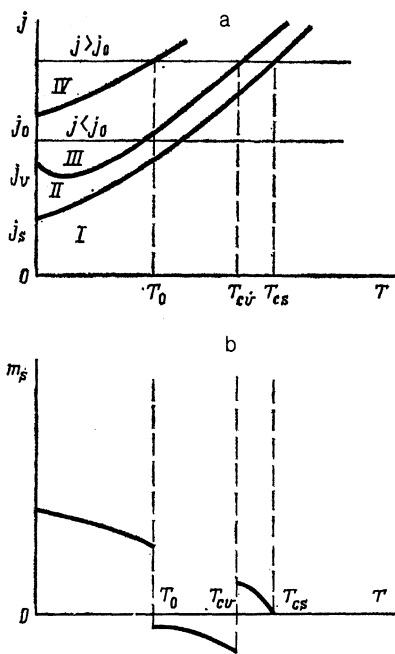


FIG. 8. a: Plots of  $j_0$ ,  $j_v$ , and  $j_s$  versus the temperature  $T$ . The Roman numerals mark the regions bounded by the curves  $j_i(T)$ . I— $m_s = 0$ ,  $m_v = 0$ ; II— $m_s > 0$ ,  $m_v = 0$ ; III— $m_s < 0$ ,  $m_v > 0$ ; IV— $m_s > 0$ ,  $m_v > 0$ . b: The surface magnetic moment  $m_s$  versus the temperature in a weak magnetic field  $h > 0$ .

$j_v(T)$  (see Fig. 6a for  $j_s < j < j_v$ ). Finally, at  $T > T_{cs}$ , the interaction  $j$  becomes weaker than  $j_s(T)$ ; i.e., the surface moment disappears.

The result is the temperature dependence of the surface moment,  $m_s(T)$ , shown in Fig. 8b. This dependence precisely reproduces the experimental behavior<sup>1</sup> of the surface moment of the alloy FeNi<sub>3</sub> (111), with one exceptional point. At  $T = T_0$ , there is a jump in the moment on the theoretical curve. Judging from the accuracy of the temperature and moment measurements in Ref. 1, that jump could not have been detected experimentally. A final answer to the question regarding the jump in the surface moment at  $T = T_0$  will have to await more-accurate measurements as well as more-detailed calculations, incorporating the crystallographic structure of the FeNi<sub>3</sub> alloy, the indices of the face, the concentration profile, etc. The qualitative picture which emerges from the simple model which we are discussing here, which systematically incorporates the evolution of the band structure as we approach the surface, probably reflects the experimental situation more accurately.

In agreement with the experimental results<sup>3</sup> on Gd (0001), the antiparallel orientation of  $m_s$  and  $m_v$  occurs at arbitrary  $T < T_{cv}$  (in Ref. 3, the lowest temperature studied was 200 K). If  $j_s, j_v < j < j_0$ , then this effect (the antiparallel orientation) formally occurs down to  $T = 0$  (Fig. 8a). This conclusion agrees qualitatively with the experimental results on Gd(0001), although the approximation of collectivized electrons is not regarded as a good approximation of the band structure of rare earths.

It is also interesting to follow the evolution of the band structure corresponding to the three solutions (1, 2, and 3 in Figs. 6 and 7) for the surface as the interaction  $j$  strengthens. When we fix the Fermi level,  $\omega_F = 6$ , we find the following results. At  $j < j_s = 0.887$ , the density of states is spin-

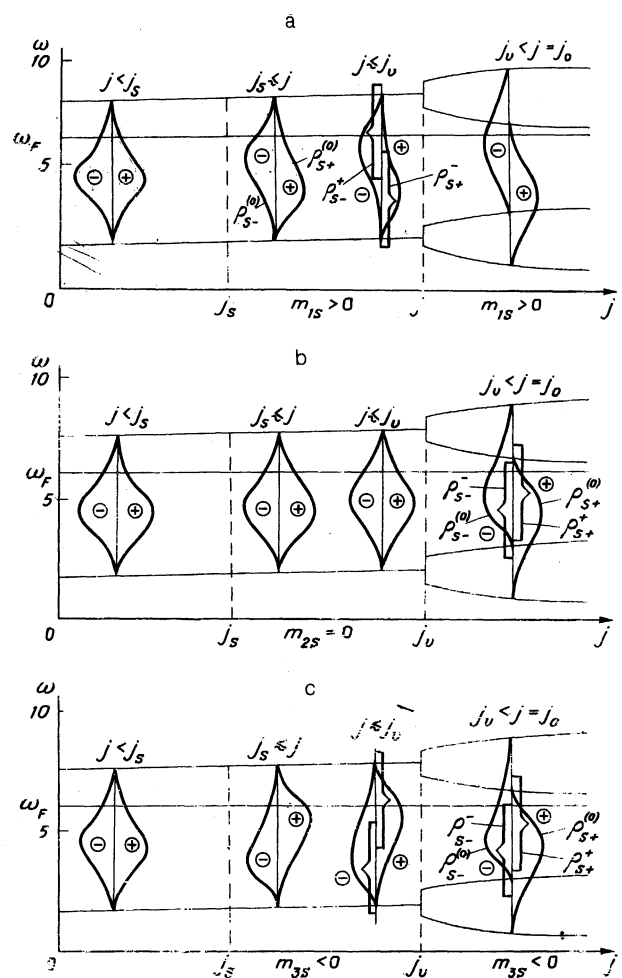


FIG. 9. The band structure of the surface corresponding to the first (a), second (b), and third (c) solutions versus the strength of the interaction.

degenerate  $\rho_{s+}(\omega) = \rho_{s-}(\omega)$ ,  $\rho_{v+}(\omega) = \rho_{v-}(\omega)$  and symmetric with respect to the middle of the band. This result is a consequence of our choice of a simple cubic lattice, which has no surface bands (Fig. 9). At  $j \geq j_s$ , in addition to solution 2 for the density of states (this solution is symmetric with respect to the middle of the band) we find two other solutions, for which there are peaks in  $\rho_{s+}(\omega)$  and  $\rho_{s-}(\omega)$  above and below the middle of the band (Fig. 9, a and c). The interval of energies  $\omega$  again coincides with the bulk interval; if  $j$  is not too large, there are no surface bands.

For the first solution in Fig. 9a,  $\rho_{s+}(\omega)$  has a peak at the bottom of the band, and  $\rho_{s-}(\omega)$  has one at the top. We thus have  $n_{1s+} > n_{1s-}$  and  $m_{1s} > 0$  (Fig. 9a). For the third solution, we find the opposite situation:  $\rho_{s+}(\omega)$  has a peak at the top of the band, and  $\rho_{s-}(\omega)$  has one at the bottom. We thus have  $n_{3s+} < n_{3s-}$  and  $m_{3s} < 0$  (Fig. 9c). With a further strengthening of the interaction,  $j \lesssim j_v = 0.92$ , the first and third solutions contain surface bands: For the first solution, a surface band  $\rho_{s-}(\omega)$  splits off from the top of the bulk band, and a surface band  $\rho_{s+}(\omega)$  splits off from the bottom, because of the relation  $|\chi_{1\pm}| > 1$  (Fig. 10a). We thus find that  $\rho_{s-}(\omega)$  shifts upward, and  $\rho_{s+}(\omega)$  downward. The number of electrons  $n_{1s+}$  become even greater than  $n_{1s-}$ , and the moment  $m_{1s}$  increases (Fig. 6a). For the third solution, in contrast, a surface band  $\rho_{s+}(\omega)$  splits off from the top of the bulk band ( $\chi_{3s+} > +1$  in Fig. 10b),

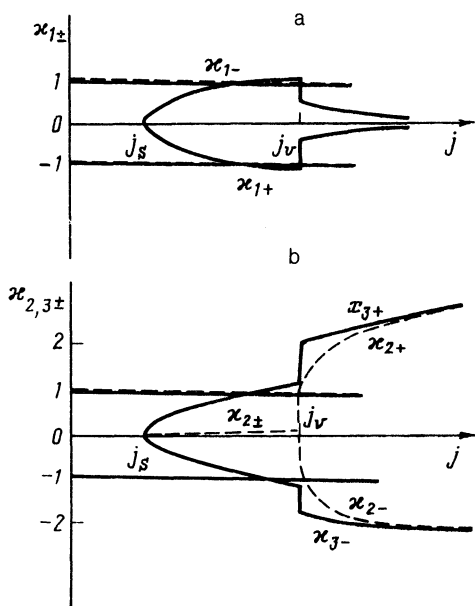


FIG. 10. Dependence of the surface perturbations  $\kappa_{\sigma} = 2g \times (n_{s-\sigma} - n_{v-\sigma})$  on the interaction  $j$  ( $g = 6j$ ). a—Corresponding to the first solution; b—corresponding to the second and third solutions.

while a surface band  $\rho_{s-}(\omega)$  splits off from the bottom ( $\kappa_{3s-} < -1$  in Fig. 10b). The negative moment  $m_{3s}$  increases in magnitude, since the number of electrons  $n_{3s-}$  increases, while  $n_{3s+}$  decreases.

At  $j < j_v$ , the surface perturbations  $\kappa_{\pm}$  for the first and third solutions are not particularly large ( $\max|\kappa_{\pm}| \approx 1.2$ ). In other words, these perturbations do not make particularly large excursions from the interval  $(-1, +1)$ . Consequently, the number of electrons in the surface bands is low, and their role negligible. The situation changes when the interaction  $j$  becomes greater than  $j_v$ , and a moment  $m_v > 0$  appears in the interior of the metal. The bulk band  $\rho_{v+}(\omega)$  shifts downward, and  $\rho_{v-}(\omega)$  upward; i.e., the changes are the same as for the surface densities of states  $\rho_{s+}^{(0)}(\omega)$  and  $\rho_{s-}^{(0)}(\omega)$ . For the first solution we have  $m_{1s} > 0$ , and the two surface bands disappear entirely (Figs. 9a and 10a), because of the relation  $|\kappa_{1\pm}| < 1$ . For the third solution (Fig. 9c), the role of the surface bands increases substantially, since  $\kappa_{3+}$  in-

creases from 1.2 to 2.1, and  $\kappa_{3-}$  decreases from  $-1.2$  to  $-1.9$  (Fig. 10b).

With a further strengthening of the interaction,  $\kappa_{3+}$  increases to  $\approx 3$ , while  $\kappa_{3-}$  remains essentially the same at  $\kappa_{3-} \approx -2$ . The top of the surface band  $\rho_{s-}(\omega)$  corresponding to the perturbation  $\kappa_{3-}$  reaches the Fermi level from below at  $j = j_0$ . At this time, the thermodynamic potentials  $\Omega_{1s}$  and  $\Omega_{3s}$  become comparable (Fig. 6b), and a first-order phase transition occurs from the third solution, with  $m_{3s} < 0$ , to the first, with  $m_{1s} > 0$ . This transition at  $j = j_0$  is accompanied by the abrupt disappearance of the surface bands  $\rho_{s-}(\omega)$  and  $\rho_{s+}(\omega)$ .

- <sup>1</sup> Yu. A. Mamaev, V. N. Petrov, and S. A. Starovoitov, Pis'ma Zh. Tekh. Fiz. **13**, 1530 (1987) [Sov. Tech. Phys. Lett. **13**, 642 (1987)].
- <sup>2</sup> D. Weller, S. F. Alvarado, W. Gudat, K. Schröder, and M. Campagna, Phys. Rev. Lett. **54**, 1555 (1985).
- <sup>3</sup> D. Weller, S. F. Alvarado, M. Campagna, W. Gudat, and D. D. Sarma, J. Less-Common Met. **111**, 277 (1985).
- <sup>4</sup> M. I. Kaganov and A. N. Omel'yanchuk, Zh. Eksp. Teor. Fiz. **61**, 1679 (1971) [Sov. Phys. JETP **34**, 895 (1971)].
- <sup>5</sup> G. Allan, Surf. Sci. Rep. **1**, 121 (1981).
- <sup>6</sup> V. D. Borman, L. A. Maksimov, and A. P. Popov, Zh. Eksp. Teor. Fiz. **90**, 697 (1986) [Sov. Phys. JETP **63**, 407 (1986)].
- <sup>7</sup> V. D. Borman, L. A. Maksimov, and A. P. Popov, Poverkhnost' No. 4, 149 (1986).
- <sup>8</sup> V. D. Borman, L. A. Maksimov, and A. P. Popov, Poverkhnost' No. 4, 5 (1988).
- <sup>9</sup> C. Rau and C. Jin, J. Appl. Phys. **63**, 3667 (1988).
- <sup>10</sup> S. Matsuo and I. Nishida, J. Phys. Soc. Jpn. **49**, 1005 (1980).
- <sup>11</sup> L. E. Klebanoff, S. W. Robey, G. Liu, and D. Shirley, Phys. Rev. B **30**, 1048 (1984).
- <sup>12</sup> H. Akoh and A. Tasaki, J. Phys. Soc. Jpn. **42**, 791 (1977).
- <sup>13</sup> H. Akoh and A. Tasaki, J. Appl. Phys. **49**, 1410 (1978).
- <sup>14</sup> C. Rau and S. Eichner, Phys. Rev. Lett. **47**, 939 (1981).
- <sup>15</sup> A. M. Bobyur', M. A. Vasil'ev, S. D. Gorodetskiĭ *et al.*, "Study of the structure of surface layers of Fe-Ni and Co-Ni single crystals" [in Russian], Preprint 14.90, Institute of the Physics of Metals, Academy of Sciences of the Ukrainian SSR, Kiev, 1990.
- <sup>16</sup> H. Hasegawa, Techn. Rep. of ISSP, Ser. A No. 4, 1585 (1985).
- <sup>17</sup> A. K. Kazanskiĭ, A. S. Kondrat'ev, and V. M. Uzdin, Zh. Eksp. Teor. Fiz. **94**(2), 274 (1988) [Sov. Phys. JETP **67**(2), 372 (1988)].
- <sup>18</sup> L. E. Klebanoff, S. W. Robey, G. Liu, and D. A. Shirley, Phys. Rev. B **31**, 6379 (1985).
- <sup>19</sup> L. E. Klebanoff, R. H. Victora, L. M. Falicov, and D. A. Shirley, Phys. Rev. B **32**, 1997 (1985).
- <sup>20</sup> D. Kalkstein and P. Soven, Surf. Sci. **26**, 85 (1971).
- <sup>21</sup> W. Schumacher, U. Lindner, and R. Jauch, Phys. Status Solidi (b) **86**, 621 (1978).

Translated by D. Parsons